Published in final edited form as:
Curr Pharm Des. 2009 ; 15(35): 4003–4016.

Unraveling the structure and function of G protein-coupled receptors through NMR spectroscopy

Irina G. Tikhonova and **Stefano Costanzi***
Laboratory of Biological Modeling, National Institute of Diabetes and Digestive and Kidney Diseases, National Institutes of Health, DHHS, Bethesda, MD 20892, USA

Abstract

G protein-coupled receptors (GPCRs) are a large superfamily of signaling proteins expressed on the plasma membrane. They are involved in a wide range of physiological processes and, therefore, are exploited as drug targets in a multitude of therapeutic areas. In this extent, knowledge of structural and functional properties of GPCRs may greatly facilitate rational design of modulator compounds. Solution and solid-state nuclear magnetic resonance (NMR) spectroscopy represents a powerful method to gather atomistic insights into protein structure and dynamics. In spite of the difficulties inherent the solution of the structure of membrane proteins through NMR, these methods have been successfully applied, sometimes in combination with molecular modeling, to the determination of the structure of GPCR fragments, the mapping of receptor-ligand interactions, and the study of the conformational changes associated with the activation of the receptors. In this review, we provide a summary of the NMR contributions to the study of the structure and function of GPCRs, also in light of the published crystal structures.

Keywords

G protein-coupled receptors (GPCRs); NMR; three-dimensional structures; ligand recognition; receptor activation

G protein-coupled receptors (GPCRs), also known as seven transmembrane-spanning receptors (7TMRs), are a large superfamily of signaling proteins expressed on the plasma membrane that function as receivers for extracellular stimuli [1]. About 1000 GPCRs have been identified in the human genome [2]. Since their signaling is involved in numerous physiological functions and pathological conditions, GPCRs constitute the molecular target of a significant percentage of the currently marketed drugs. Moreover, many additional members of the superfamily have been identified as potential targets for the treatment of a variety of diseases and are the object of substantial drug discovery efforts. From the molecular point of view, all GPCRs share a common molecular architecture, being composed of a single polypeptide chain folded into a bundle of seven α-helical transmembrane domains (TMs) connected by three extracellular and three intracellular loops (ELs and ILs). The N-terminus is located in the extracellular space, while the C-terminus is in the cytosol (Fig. (1)).

Given that structure-based drug discovery is an efficient method to rationally design novel drugs and improve the properties of old drugs, the scientific community has been striving for a long time to shed light onto the elusive structure-function relationships of GPCRs employing a variety of direct biophysical and indirect biochemical methods [3]. The most direct method that has been used is X-ray crystallography. However, up until now, this technique has been

*address for correspondence: stefanoc@mail.nih.gov.

applied successfully only to a limited number of receptors, namely rhodopsin, the unliganded opsin, the beta-adrenergic receptors (β-ARs), and the adenosine A_{2A} receptor [4–13]. In particular, the low resolution projection map of bovine rhodopsin published by Schertler in 1993 [14] and the subsequent 2.8 Å resolution structure published by Paczewski in 2000 [15] provided the first static three-dimensional (3D) pictures of a GPCR, and have been widely used as templates for the construction of homology models. The subsequent recent publication of the X-ray structure of the β-ARs and the A_{2A} receptor [6;7;10;11] proved conclusively that GPCRs share a common arrangement of the TMs, while suggesting a greater variability for the extracellular and intracellular regions. This includes the second extracellular loop (EL2), which, together with the portions of the TMs facing the extracellular side, is thought to line the ligand binding pocket for the great majority of GPCRs.

On the basis of the available crystallographic information, various studies reported insights into the structure and functions of GPCRs obtained through indirect methods such as site-directed mutagenesis, zinc crosslinking of histidines, photoaffinity labeling and site-specific chemical labeling (see as examples [16–22]). In this context, in silico molecular modeling conducted in an iterative manner with the gathering of experimental data became a widespread tool to infer the 3D structure of the receptors [23–25]. Like other researchers, we have successfully applied this approach to the identification of modulators of several GPCRs (see as examples [26–29]). Despite the relatively low sequence identity between rhodopsin and most other GPCRs, which instilled many doubts on the reliability and the scope of rhodopsin-based modeling, a recent comparison between in silico models and X-ray structure of theβ_2-AR firmly supported the applicability of homology modeling and molecular docking to the study of GPCR/ligand complexes [30].

Besides crystallography, other direct methods of investigation aimed at gathering atomic-resolution information have been also applied, among which electron crystallography, electron paramagnetic resonance, UV absorbance and fluorescence spectroscopy, and, as we will discuss at length in this review, nuclear magnetic resonance (NMR) spectroscopy (see as examples [14;31–38]).

NMR spectroscopy, conducted in solution or in solid-state, is a powerful method to study protein structure, protein dynamics, and protein-ligand interactions. NMR techniques are routinely used in drug discovery for soluble protein targets [39;40]. Although their application to GPCRs is hindered by difficulties related to the preparation of receptor samples and the interpretation of the complex spectra, many studies directed towards a structural characterization of GPCRs through NMR have been reported, providing useful information for structure-based drug discovery.

The methods and technical challenges underlying the application of NMR spectroscopy to membrane proteins and GPCRs have been covered in recently published reviews [41–43]. Here, we will focus on the advances in the understanding of the structure and function of GPCRs that have been made through NMR studies. In particular, the review is divided in three sections: in the first one, we will discuss attempts to determine 3D structures of GPCRs; in the second one, we will illustrate studies on receptor-ligand interactions conducted by labeling ligands and/or selected residues in the binding pocket; in the third section we will review studies intended to elucidate the motions and the structural changes consequent to the activation of the receptor, also conducted by labeling selected receptor residues.

1. Determination of the 3D structure of GPCRs

Many obstacles interfere with the determination of the complete 3D structure of a GPCR. Structural studies by NMR require the assignment of all resonance picks in the spectra. Since ^1H is the only NMR active isotope abundantly present in proteins, a complete assignment

of the complex NMR spectra for a whole protein the size of a GPCR is contingent to the preparation of protein samples uniformly labeled with NMR active C and/or N isotopes.

NMR spectra are complicated by anisotropic nuclear spin interactions, such as dipole-dipole coupling, chemical shielding anisotropy, and quadrupole coupling. Solution-state NMR, which takes advantage of the averaging effect on anisotropic interactions due to the fast tumbling of the samples, is routinely applied to the analysis of proteins with a molecular weight between 30 and 50 kDa. Solid-state NMR spectra, ideal for membrane proteins such as GPCRs, are complicated by the restricted molecular movements that prevent the averaging of the anisotropic effects, inducing a peak-broadening that lowers significantly the resolution of the spectra [42;43].

The introduction of the magic-angle spinning and oriented-sample techniques substantially addressed these problems. However, the complexity of the solid-state NMR spectra and difficulties related to sample preparation have prevented, so far, the solution of the structure of whole GPCRs through NMR. For these reasons, most of the studies have been directed toward the solution of individual portions of the receptor structure either in aqueous solution or in different lipid-mimetic solvents [41]. In Table 1, we report a synoptic view of the available 3D structural data. Additionally, for the NMR-derived GPCR fragments with 3D coordinates available in the Protein Data Bank, we provide, in Fig. (2) and (3), a structural alignment with the X-ray structure of rhodopsin and the β-ARs.

Transmembrane domains

We now know from crystallographic data that some of the TMs present kinks in their α-helical structures, particularly pronounces in TM6 and TM7. These data emerged clear from NMR studies, even before the publication of GPCR X-ray structures. In particular, kinks were detected studying portions of TM6 of the *Saccharomyces cerevisiae* α-factor receptor (Ste2pR) [44] and TM7 of the tachykinin receptor NK_1 [45] (Table 1). Solution and solid-state NMR studies of the TMs of the Ste2pR continued after the disclosure of the X-ray structure of rhodopsin and, among other findings, confirmed the existence of the helical kink of TM6 previously detected through solution NMR with the a more sophisticated solid-state NMR of the ^{15}N labeled TM6 peptide in 1,2-dimyristoyl-sn-glycero-phosphocholine bilayers [46–49]. As mentioned, the kinks of TM6 and TM7 postulated on the basis of the NMR results are consistent with the conformation of the homologous regions of the receptors that have now been crystallized (Fig. (2), panel A) [12;15], supporting the idea that even structural data gathered for isolated domains can be very informative. Probably, even greater insights could be obtained from the analyses of larger substructures or even whole receptors. At this purpose, Zheng and coworkers biosynthesized a quite large segment of the cannabinoid CB_2 receptor, including TM1, IL1 and TM2, using a fusion protein overexpression strategy [50]. The preliminary results gathered by the authors for the $^{13}C/^{15}N$ labeled peptide argue in favor of the applicability of this strategy to the synthesis of GPCR helical bundles for NMR studies.

Extracellular loops

While homology modeling based on the available GPCR X-ray structures allows the construction of reliable models of the TMs, modeling the 3D structure of extracellular and intracellular regions remains a difficult task [30]. Low sequence similarity as well as numerous insertions and deletions, hamper an effective application of homology modeling to these regions. NMR spectroscopy could prove particularly useful in solving this problem: the structures of loops and termini of the receptor of interest could be derived through NMR and subsequently combined with homology models to build complete 3D structures.

To obtain structures of ILs and ELs close to the naturally occurring ones, many experimentalists turned to the application of structural constraints meant to keep the termini at a distance compatible with their role of connecting two TMs. In some cases, portions of the adjacent TMs have been added to act as anchors for shackling loops or termini to the lipid environment. Alternatively, the loops have been constrained with disulfide bridges between cysteines [51] or S-carboxymethylcysteines [52] added to the peptide termini, with or without methylene linkers [53].

Since for most of the GPCRs activated by peptides ligand binding is thought to occur at the level of the extracellular domains, NMR analyses have been extensively applied to study receptor-peptide interactions. For example, the contact interactions of CCK8–the natural cholecystokinin peptide, composed of eight amino acids–with the N-terminus and EL3 of the CCK_1 and with EL3 of the CCK_2 subtypes of the cholecystokinin receptors have been studied by NMR by monitoring chemical shift perturbations and intermolecular NOEs [54–56] (Table 1). For the CCK_2 the analysis has been complemented by integrating NMR-derived structural information with rhodopsin-based homology modeling. With a similar strategy, the interactions between the CCK_1 and synthetic agonists have also been studied [57]. The integration of homology modeling and NMR-derived information provided also a structural hypothesis for the binding of substance P to the NK_1 receptor, confirming and rationalizing the results previously obtained through a variety of indirect biochemical methods [58]. A similar approach also corroborated the postulated existence of a disulfide bridge between EL1 and EL2 in the thromboxane A_2 receptor (TP), highlighting also the involvement in ligand binding of the WCF motif of EL2 [59;60].

Lastly, Pham and coworkers developed an alternative methodology for studying GPCR loops based on the computational design of a peptide containing segments that mimic the self assembling of the ends of two TMs connected by the loop under examination [61]. When applying their strategy to the analyses of EL1 of the sphingosine 1-phosphate receptor S_1P_4, the authors obtained the best results with the coiled-coil strategy, i.e. by substituting the TM2 and TM3 segments with sequences from structurally characterized water-soluble proteins with a pair of antiparallel helices oriented in a way consistent with the S_1P_4 homology model. The addition of a disulfide bridge appeared also necessary to keep the helices together. The ability of the peptide to bind an analog of the agonist's headgroup suggested that EL1 adopted a biologically relevant conformation. Here, we superimposed this NMR-derived structure to the homologous regions in the crystal structure of the β_2 receptor (Fig. (2), panel A) and, in agreement with the conclusions of the authors, revealed a sensible conformation and orientation for the TM2 and TM3 mimetics.

Intracellular loops

Since the ILs, and IL2 in particular, are directly involved in the coupling of the receptors with the G proteins, [62–64] the experimental elucidation of the structure of these binding interfaces would provide insights into the molecular mechanisms of the selectivity toward the various G protein subtypes.

NMR studies of IL2 in the adrenergic α_{2A} receptor, rhodopsin, the bradykinin B_2 receptor, and the vaspressin V_{1a} receptor have been performed (Table 1) [52;65;66]. In particular, NMR studies of the peptide corresponding to the IL2 of theα_{2A} receptor revealed the presence of a cytoplasmic helix not detected in the analogous rhodopsin peptides [65] or in the crystal structure of rhodopsin. X-ray crystallography revealed that this helix, although not detected in the β_2, is indeed present in the β_1 subtype [7;11].

Conversely, the NMR-derived structure of IL2 of the B_2 receptor revealed a "U" shape [66] similar to that detected in rhodopsin. Also in the case of the vasopressin V_{1A} receptor, the

NMR analysis of a linear and a cyclic IL2 peptide revealed a conformation in TFE/H_2O solvent similar to that shown in rhodopsin, particularly with the cyclic peptide [52].

The structure of IL3 has also been determined for several receptors, including the cannabinoid CB_1 receptor, the β_2 receptor, and the parathyroid hormone PTH1 receptor (Table 1) [53;67;68]. Of note, the IL3 peptide of the CB_1 receptor (Fig. (2), panel A) assumed a helical conformation in aqueous solution when $G\alpha_{i1}$ was added, while a mutated IL3 formed just a single helixturn [68]. The authors proposed the importance of this portion of IL3 in the formation of the G protein binding interface.

Also for the ILs, hybrid solutions composed of molecular modeling and NMR studies have been applied. In particular, Wu and coworkers derived by NMR the structure of all three ILs of the thromboxane A_2 receptor and subsequently incorporated them into a rhodopsin-based homology model [51]. They consequently proposed a list of amino acid residues potentially involved in the formation of the G protein-binding interface that proved consistent with available mutagenesis data.

N-/C- termini

In addition to the mentioned NMR structure of the CCK_1 N-terminus, the structure of the N-terminus of PTH1 receptor has also been solved [69], revealing to be different from that of rhodopsin (Fig. (2), panel A). These data confirm the idea that each GPCR may be characterized by unique extracellular regions that contribute to the selectivity of the receptors for specific ligands.

All the available GPCR X-ray structures are characterized by the presence of aα-helix, known as helix 8 (H8), in the portion of the C-terminus proximal to TM7. NMR in conjunction with CD spectroscopy confirmed the presence of an H8 for the CB_1 andCB_2 receptors, the Ste2p receptor, the $\beta_1$and β_2 receptors, the angiotensin AT_{1A} receptor, and the bradykinin B_2 receptor in detergent [70–75]. In Fig. (2), panel B, we superimposed the NMR-derived the β_1 receptor H8 to the corresponding segment of the crystal structure of the same receptor, revealing a very good agreement between crystallographic and NMR data. Conversely, a random coil conformation was detected in water for this region [71–73]. These conformational changes of H8 have been speculated to be indicative of possible structural rearrangements consequent the activation of the receptors. For instance, partial unfolding of H8 upon light activation has been detected in rhodopsin by Fourier transform infrared (FTIR) and fluorescence spectroscopy [76].

Several NMR studies of the rhodopsin C-terminus have been published [33;77;78]. Beyond H8, this region resulted unstructured in aqueous solution, both in unphosphorylated or phosphorylated form, while has adopted a defined 3D structure when phosphorylated and in the presence of arrestin (Fig. (2), panel C) [78]. Here we could only compare this NMR-derived structure (pdb code: 1nzs) with the crystal structures of lumirhodopsin and batorhodopsin (pdb code: 2hpy and 2g87), for which this distal portion of the C-terminus has been determined. The detected fairly high root mean square deviations of 5.5–6 Å suggest that the C-terminus of rhodopsin undergoes a conformational change when bound to arrestin.

Yeagle's approach to derive the structure of rhodopsin through NMR

Before the obtainment of high resolution X-ray structures of GPCRs, Yeagle and coworkers devised a methodology intended to solve the 3D structure of portions of the receptors and subsequently assemble them together. Through two dimensional homonuclear ^1H NMR analyses in solution, the authors determined the structure of overlapping peptides spanning the entire sequence of the rhodopsin and subsequently computationally assembled the fragments

into a single structure [79–81]. The information about the packing of the helical bundle, necessary to put the pieces together, was gathered from electron paramagnetic spectroscopy (EPS) [36;82;83], zinc crosslinking of histidines [16], and electron cryo-microscopy data [84]. In the form of distance constraints, this was then applied to the NMR-derived fragments through simulated annealing. Using different sets of experimental data collected for the ground-state and activated (META II) rhodopsin, the authors intended to generate models for both states (PDB codes: 1jfp and 1ln6). After the publication of the crystal structure of rhodopsin, the authors discovered that the largest TM peptides yielded the best superimposition with the corresponding segments of the crystal structure [85].

Here we superimposed Yeagle's ground state rhodopsin to the crystal structures of the ground state rhodopsin (PDB code: gzm), detecting a RMSD of the backbone of about 6 Å (Fig. (3), panel A). The packing of the TM helical bundle is similar in the two structures, however, Yeagle's model predicts the presence of several non helical portions, in particular in TM7, not confirmed by the crystallography. The intracellular and extracellular regions appear significantly divergent in the Yeagle's model and the crystal structure. We also superimposed Yeagle's Meta II rhodopsin to the recently solved crystal structure of opsin in its G protein interacting conformation [8], detecting, also in this case, an RMSD of the backbone of about 6 Å (Fig. (3), panel B).

Whole GPCRs

Dispite the difficulties, several attempts to solve the structure of whole GPCRs by NMR are currently being undertaken. Solution NMR spectroscopy experiments, conducted for the uniformly ^{15}N-labelled vasopressin V_2 receptor, solubilized with lyso-myristoylphosphatidylcholine, indicated the potential suitability of the technique for structural studies of GPCRs. Notably, the authors observed over 250 amide peaks out of the expected 349 in their ^{1}H,^{15}N-TROSY spectrum [86]. Additionally, solid-state NMR studies of a uniformly ^{15}N-labeled and selectively ^{15}N-Ile-labeled chemokine CXCR1 receptor in magnetically aligned bicelles provided spectra that suggested the potential applicability of NMR to structural determinations and the elucidation of structure-activity relationships (vide infra) [32].

2. Mapping receptor-ligand interactions

Direct atomic resolution information on the interactions of GPCR with their ligands is available through X-ray crystallography only for a limited number of receptors, while, for the great majority of them, indirect methods of analysis have been used. A synergistic application of mutagenesis studies, photoaffinity labeling, chemical modifications of the ligands, and computational modeling has been the most common way of studying the determinants of ligand recognition. Taken together, these results have contributed to the general definition of a common binding pocket for GPCRs located towards the extracellular opening of the helical bundle [87;88]. Also for receptors naturally stimulated by ligands that bind to their N-terminal ectodomains, such as the calcium sensing or the glycoprotein hormone receptors, the possibility of modulation through ligands that bind within their helical bundle has been demonstrated [89–93].

In this context, structure-activity relationships (SAR) analyses and drug-discovery studies would greatly benefit from direct experimental proofs of receptor-ligand interactions, such as those that NMR could provide. Solid-state NMR spectroscopy has been applied successfully to membrane proteins to detect ligand binding and to analyze protein-ligand interactions, especially when coupled to selective isotopic labeling of specific residues located in the binding pocket and/or of the ligand [94]. Through this expedient, significantly simplified spectra with a manageable amount of signals have been obtained, thus rendering NMR applicable to the

analysis of bioactive ligand conformations, protonation states, receptor/ligand interactions and residue/residue interactions. Moreover, although not yet for GPCRs, NMR coupled to selective isotopic labeling has successfully been applied to rational fragment-based drug discovery. In particular, ligands or fragments that bind to specific pockets of a protein have been identified by monitoring the changes in the chemical shifts of ^{15}N or ^{1}H-amide atoms in ^{15}N-labelled protein, an approach known as SAR by NMR [95;96].

Rhodopsin has been extensively studied by solid-state NMR coupled to selective labeling. Before any high-resolution crystal structures were released, selective ^{15}N-labeling of Lys residues led to the conclusion that the distance between the protonated Schiff base by which the retinylidene chromophore is covalently bound to K296(7.43 according to the Ballesteros and Weinstein residue indexing [97]) and the E113(3.28) counterion (Fig. (4)) was greater than 4 Å [98]. The subsequent publication of crystal structures, revealed that the distance is, in fact, about 3.5 Å.

The conformation of retinal and its interactions with rhodopsin have also been studied extensively through NMR coupled to selective labeling. For example, high-resolution solid state deuterium (^{2}H) NMR experiments provided detailed information on the orientation of retinal in the binding pocket and on the conformational changes that occur with the transition from the ground state to the Meta I intermediate of the activation cycle. The study applied three retinal analogues labeled with deuterium at three different pairs of adjacent carbons [99]. Ultra high field solid-state magic angle spinning 2D homonuclear and 2D heteronuclear NMR spectroscopy has also been used to study rhodopsin reconstituted with a uniformly ^{13}C-labeled 11-cis-retinal. Complete assignment of the ^{13}C and ^{1}H chemical shifts for retinal highlighted nonbonding interactions between the protons of the methyl groups of its ionone ring and the nearby aromatic acid residues F208(5.43), F212(5.47), and W265(6.48) (Fig. (4)). Furthermore, it was shown that binding of retinal involves a chiral selection of the ring conformation, resulting in equatorial and axial positions for CH_3-16 and CH_3-17 [100]. Additional evidences of the interactions between retinal and rhodopsin in the ground and Meta I states have also been obtained through NMR experiments conducted variously labeling the ligand with ^{2}H [101–104]. These data support the hypothesis that a strain in the polyen around the *cis* bond assists the photoisomerization of retinal. A ^{13}C-labelled 9-cis retinal isomer, typical of isorhodopsin, has also been investigated, leading to similar conclusions [105].

Application to rhodopsin of an NMR technique named by the authors “selective interface detection spectroscopy” (SIDY), based on the detection of the correlations between ^{13}C atoms of labeled ligands and ^{1}H atoms of unlabelled receptors, led to the detection of several contacts between the aliphatic carbons of the 11-*cis*-retinal ionone ringand residues in the binding pocket. Although, SIDY data do not provide sequence-specific assignments of the contacts, these could be identified by means of additional data, and, in the case of rhodopsin, resulted in good agreement with the available crystallographic structures [106].

NMR spectroscopy provides also a very effective way of studying the conformational changes that a ligand undergoes upon binding to a receptor. In this context, the analysis of the unbound and receptor-bound ^{13}C,^{15}N-labelled neurotensin, a 13-residue peptide, revealed that the ligand is in a disordered state in the absence of the receptor, while adopts a beta-strand conformation when bound to the NTS_1 receptor [107]. Similarly, the structure of the bradykinin (BK) peptide bound to the bradykinin B_2 receptor has been studied through solid-state NMR, revealing a double S-shape structure [108]. These type of studies can be also conducted to rationalize the biological activities of compounds on the basis of their bioactive conformations, as it has been done in the case of two natural peptides active at the neuropeptide NPR-1 receptor one [109].

In addition to conformational changes, NMR spectroscopy can also detect changes in the protonation state of a ligand as a consequence of binding to a receptor. In this context, solid state NMR experiments conducted with uniformly labeled ^{13}C,^{15}N-histamine bound to the human histamine H_1 receptor revealed that the ligand can bind either in a monocationic or a dicationic form. On the basis of their data, the authors hypothesized that, in analogy with rhodopsin, also in the case of the H_1 receptor a protonation switch might be part of the activation mechanism [110].

3. Detection of motions and conformational changes associated with receptor activation

Upon binding of agonists, which typically occurs in proximity of the extracellular opening of the helical bundle, GPCRs undergo a series of structural changes that cascade from the extracellular to the intracellular part of the receptor and ultimately lead to G protein activation. Detailed structural knowledge of the ground and activated state of the receptor and mechanistic insights into the activation process would significantly assist drug discovery, allowing a more rational design of compounds capable of stimulating or blocking the receptor.

A wealth of information has been derived by the analysis of mutations that affect the basal activity of GPCR, either naturally occurring or generated through site-directed mutagenesis. Mutations that cause an increase of the basal activity are likely to stabilize the activated state of the receptor and are referred to as constitutively active mutants. Those that prevent the activation of the receptor are, instead, called uncoupling mutants and are likely to stabilize its inactive state or to disrupt the cascade of conformational changes that lead to signaling. Through such mutational analyses, various molecular switches for GPCR activation have been proposed [111;112]. Alternatively, the structural changes that occur upon receptor activation have been monitored through electron paramagnetic resonance spectroscopy (EPR) [34;36; 83;113], UV absorbance spectroscopy [35], engineering of metal-ion-binding sites [16], as well as site-specific chemical labeling coupled to fluorescence spectroscopy [37], and, as we will see in the coming paragraphs, NMR spectroscopy. These data shed light onto a number of intramolecular distances that are characteristic of the activated receptors. We recently used these biophysically measured distances to construct a computational structure of the activated rhodopsin based on coarse-grained and all atom simulations, and subsequently study the dynamics of the activation process [114]. The substantial conformational changes predicted by these indirect methods were not detected in the crystal structure of a photoactivated deprotonated intermediate (PDI) of rhodopsin that shows absorption maxima consistent with the META II state [13]. The crystal lattice may have prevented large-scale structural rearrangements. However, a significant opening of the intracellular surface of the receptor and a furthering of the intracellular ends of TM3 and TM6 have been captured in the crystal structure of opsin with a fragment of the C-terminus of transducin. At least relatively to the cytosolic half, this may represent the first detailed structure of an activated GPCR [8].

Compared to crystallography, NMR spectroscopy offers the possibility of conducting structural analyses in a less constrained membrane-like environment. In this context, NMR is well suited to the study of receptor activation through isotopic labeling of specific residues located in areas affected by the structural changes. In this context, the specific labeling of rhodopsin led to observance of the transition between its inactive and activated states.

2D-dipolar-assisted rotational resonance NMR measurements between ^{13}C-labels on the C14, C15, C19, C20 atoms of retinal and ^{13}C-labeled G114(3.29), T118(3.33), G121(3.36), Y178 (4.68), G188(EL2), Y191(EL2), S196(EL2), and Y268(6.51), all located in the retinal binding pocket, was performed for the ground state and META II rhodopsin (Fig. (5), panel A, purple and green spheres indicate retinal and rhodopsin atoms, respectively) [115]. The results

highlighted that the extracellular portion of the receptor undergoes conformational changes upon activation. In particular, a large rotation of the C20 methyl group of retinal toward EL2 and also a translation of about 4–5 Å of the retinal chromophore toward TM5 were observed. This displacement of retinal has been associated with the motions of the TM5, TM6, and TM7 predicted by different biophysical and biochemical methods [115]. Subsequent measurements between the C19 and C20-methyl groups of retinal and ^{13}C-labeled W265(6.48) confirmed that, in agreement with what suggested by atomic microscopy [38], the movement of the beta-ionon ring causes a reorientation of the side chain of W265(6.48) upon activation (Fig. (5), panel A, a blue sphere indicates W265). In agreement with what seen in the crystal structure of opsin [8], the study also suggested that TM6, but not TM3, undergoes a significant rearrangement [116]. Most likely, the local movements triggered by the isomerization of retinal cause a perturbation of the complex network of hydrogen bonds that stabilizes the helical bundle of the ground state rhodopsin. This is suggested also by the comparison of the chemical shifts of ^{15}N and ^{13}C-labeled wild type and mutant rhodopsin in the ground and META II states [117], which, among other observations, led to the detection of the disruption of the strong hydrogen bond between Glu 122 in TM3 and H211 in TM5 (Fig. (5), pink spheres indicate Glu122 and H211), thus indicating a motion of TM5. A more recent study demonstrated that the transition to META II is accompanied also by a displacement of EL2 from the retinal binding site, and suggested that this displacement is coupled to the rotation of TM5 and the breakage of the ionic lock connecting TM3 and TM6 [118]. As mentioned, all these interconnected conformational changes caused by the photoisomerization of retinal eventually cascade down towards the cytosolic portion of the TMs, thus leading to G protein activation. To specifically monitor the changes that occur in this region, NMR spectroscopy of ^{19}F labeled rhodopsin has been applied after mutation of specific residues to Cys and subsequent attachment of trifluoroethylthio groups via disulfide bridges (C65, C139, C140, C251, C316, indicated by yellow spheres in Fig. (5), panel A). The results support the idea that the tertiary structure of the cytoplasmic face of the receptor changes significantly upon light activation [119;120].

Beyond the activation process, NMR analyses of ^{15}N labeled rhodopsin have been applied also to the study of the dynamics of the dark adapted receptor. In particular, a study on α-^{15}N-Lys-labeled rhodopsin revealed that, while the single Lys residue located in the C-terminus is endowed with nanosecond scale movements, those located in different regions of the receptors present micro- to millisecond timescale motions (Fig. (5), panel B). In contrast with Lys residues, which in rhodopsin are located mostly in the cytosolic domains, Trp residues are, for the most part, present in the TMs (Fig. (5), panel B). A subsequent study of α and ε-^{15}N-Trp-labeled rhodopsin, confirmed that there are micro- to millisecond timescale backbone motions in the inactive dark state, while suggesting a substantial restriction of the Trp side chains to a single specific conformation [121;122].

Conclusion

Despite the numerous technical challenges, NMR spectroscopy has the potential of becoming a leading technique in the study of the structure-function relationships of GPCRs and their interactions with ligands. In contrast to crystallographic methods, which provide high-resolution but static molecular snapshots, NMR techniques can provide dynamic pictures of receptor structures and receptor-ligand interactions, thus offering insights into the molecular mechanisms of ligand recognition and receptor activation.

Through this article, we reviewed many of the contributions that NMR studies have given to the understanding of the molecular structure and functioning of GPCRs. In particular, NMR spectroscopy has been extensively applied to the study of individual portions of GPCRs, also in combination with homology modeling. Through selective labeling of ligands and/or specific

receptor residues, NMR studies have also been applied to the study of GPCR-ligand interactions and to the investigations of the molecular changes coupled to activation of the receptor.

Recently, dynamic nuclear polarization (DNP), a technique intended to increase the NMR sensitivity by transferring the polarization of electron spins to nuclei, has been successfully applied to the study the photocycle of bacteriorhodopsin, a 7TM light-driven ion pump with some structural analogies to rhodopsin [123]. Due to the enhanced sensitivity of the experiments, DNP allows the analysis of low concentration samples in a lower timeframe, and the detection of low populated conformations.

The introduction of DNP, as well as other advances in solution and solid-state NMR technology, together with progresses in the preparation of GPCR samples, are expected to lead in the future to the determination of the 3D structure of whole GPCRs, and to provide further mechanistic insights into the complex cascade of motions and rearrangements characteristic of the activation process. Furthermore, these methodological advances are also likely to foster the application of SAR by NMR techniques to the discovery of lead compounds for GPCRs through NMR-based high throughput screenings and their subsequent structure-based optimization.

Acknowledgments

This research was supported by the Intramural Research Program of the NIH, National Institute of Diabetes and Digestive and Kidney Diseases.

References

1. Pierce KL, Premont RT, Lefkowitz RJ. Seven-transmembrane receptors. Nature Reviews Molecular Cell Biology 2002;3:639–650.
2. Takeda S, Kadowaki S, Haga T, Takaesu H, Mitaku S. Identification of G protein-coupled receptor genes from the human genome sequence. Febs Letters 2002;520:97–101. [PubMed: 12044878]
3. Yeagle PL, Albert AD. G-protein coupled receptor structure. Biochimica et Biophysica Acta-Biomembranes 2007;1768:808–824.
4. Li J, Edwards PC, Burghammer M, Villa C, Schertler GF. Structure of bovine rhodopsin in a trigonal crystal form. J Mol Biol 2004;343:1409–1438. [PubMed: 15491621]
5. Okada T, Sugihara M, Bondar AN, Elstner M, Entel P, Buss V. The retinal conformation and its environment in rhodopsin in light of a new 2.2 Å crystal structure. J Mol Biol 2004;342:571–583. [PubMed: 15327956]
6. Jaakola VP, Griffith MT, Hanson MA, Cherezov V, Chien EY, Lane JR, et al. The 2.6 Angstrom Crystal Structure of a Human A2A Adenosine Receptor Bound to an Antagonist. Science 2008;322:1211–7. [PubMed: 18832607]
7. Warne T, Serrano-Vega MJ, Baker JG, Moukhametzianov R, Edwards PC, Henderson R, et al. Structure of a beta(1)-adrenergic G-protein-coupled receptor. Nature 2008;454:486–4U2. [PubMed: 18594507]
8. Scheerer P, Park JH, Hildebrand PW, Kim YJ, Krauss N, Choe HW, et al. Crystal structure of opsin in its G-protein-interacting conformation. Nature 2008;455:497–U30. [PubMed: 18818650]
9. Park JH, Scheerer P, Hofmann KP, Choe HW, Ernst OP. Crystal structure of the ligand-free G-protein-coupled receptor opsin. Nature 2008;454:183–U33. [PubMed: 18563085]
10. Cherezov V, Rosenbaum DM, Hanson MA, Rasmussen SG, Thian FS, Kobilka TS, et al. High-resolution crystal structure of an engineered human beta2-adrenergic G protein-coupled receptor. Science 2007;318:1258–1265. [PubMed: 17962520]
11. Rosenbaum DM, Cherezov V, Hanson MA, Rasmussen SG, Thian FS, Kobilka TS, et al. GPCR engineering yields high-resolution structural insights into beta2-adrenergic receptor function. Science 2007;318:1266–1273. [PubMed: 17962519]

12. Rasmussen SG, Choi HJ, Rosenbaum DM, Kobilka TS, Thian FS, Edwards PC, et al. Crystal structure of the human beta2 adrenergic G-protein-coupled receptor. Nature 2007;450:383–387. [PubMed: 17952055]
13. Salom D, Lodowski DT, Stenkamp RE, Le TI, Golczak M, Jastrzebska B, et al. Crystal structure of a photoactivated deprotonated intermediate of rhodopsin. Proc Natl Acad Sci U S A 2006;103:16123–16128. [PubMed: 17060607]
14. Schertler GFX, Villa C, Henderson R. Projection Structure of Rhodopsin. Nature 1993;362:770–772. [PubMed: 8469290]
15. Palczewski K, Kumasaka T, Hori T, Behnke CA, Motoshima H, Fox BA, et al. Crystal structure of rhodopsin: A G protein-coupled receptor. Science 2000;289:739–745. [PubMed: 10926528]
16. Sheikh SP, Zvyaga TA, Lichtarge O, Sakmar TP, Bourne HR. Rhodopsin activation blocked by metal-ion-binding sites linking transmembrane helices C and F. Nature 1996;383:347–350. [PubMed: 8848049]
17. Marco E, Foucaud M, Langer I, Escrieut C, Tikhonova IG, Fourmy D. Mechanism of activation of a G protein-coupled receptor, the human cholecystokinin-2 receptor. J Biol Chem 2007;282:28779–28790. [PubMed: 17599907]
18. Tan YV, Couvineau A, Murail S, Ceraudo E, Neumann JM, Lacapere JJ, et al. Peptide agonist docking in the N-terminal ectodomain of a class II G protein-coupled receptor, the VPAC1 receptor - Photoaffinity, NMR, and molecular modeling. Journal of Biological Chemistry 2006;281:12792–12798. [PubMed: 16520374]
19. Dawson ES, Henne RM, Miller LJ, Lybrand TP. Molecular models for cholecystokinin-A receptor. Pharmacology & Toxicology 2002;91:290–296. [PubMed: 12688371]
20. Turek JW, Halmos T, Sullivan NL, Antonakis K, Le Breton GC. Mapping of a ligand-binding site for the human thromboxane A(2) receptor protein. Journal of Biological Chemistry 2002;277:16791–16797. [PubMed: 11877412]
21. Hoffmann C, Gaietta G, Bunemann M, Adams SR, Oberdorff-Maass S, Behr B, et al. A FlAsH-based FRET approach to determine G protein - coupled receptor activation in living cells. Nature Methods 2005;2:171–176. [PubMed: 15782185]
22. Kristiansen K. Molecular mechanisms of ligand binding, signaling, and regulation within the superfamily of G-protein-coupled receptors: molecular modeling and mutagenesis approaches to receptor structure and function. Pharmacology & Therapeutics 2004;103:21–80. [PubMed: 15251227]
23. Moro S, Spalluto G, Jacobson KA. Techniques: Recent developments in computer-aided engineering of GPCR ligands using the human adenosine A(3) receptor as an example. Trends in Pharmacological Sciences 2005;26:44–51. [PubMed: 15629204]
24. Moro S, Deflorian F, Bacilieri M, Spalluto G. Ligand-based homology modeling as attractive tool to inspect GPCR structural plasticity. Current Pharmaceutical Design 2006;12:2175–2185. [PubMed: 16796562]
25. Patny A, Desai PV, Avery MA. Homology modeling of G-protein-coupled receptors and implications in drug design. Current Medicinal Chemistry 2006;13:1667–1691. [PubMed: 16787212]
26. Tikhonova IG, Sum CS, Neumann S, Thomas CJ, Raaka BM, Costanzi S, et al. Bidirectional, Iterative Approach to the Structural Delineation of the Functional “Chemoprint” in GPR40 for Agonist Recognition. J Med Chem 2007;50:2981–2989. [PubMed: 17552505]
27. Engel S, Skoumbourdis AP, Childress J, Neumann S, Deschamps JR, Thomas CJ, et al. A virtual screen for diverse ligands: discovery of selective g protein-coupled receptor antagonists. Journal of the American Chemical Society 2008;130:5115–5123. [PubMed: 18357984]
28. Kellenberger E, Springael JY, Parmentier M, Hachet-Haas M, Galzi JL, Rognan D. Identification of nonpeptide CCR5 receptor agonists by structure-based virtual screening. Journal of Medicinal Chemistry 2007;50:1294–1303. [PubMed: 17311371]
29. Tikhonova IG, Sum CS, Neumann S, Engel S, Raaka BM, Costanzi S, et al. Discovery of novel Agonists and antagonists of the free fatty acid receptor 1 (FFAR1) using virtual screening. Journal of Medicinal Chemistry 2008;51:625–633. [PubMed: 18193825]

30. Costanzi S. On the Applicability of GPCR Homology Models to Computer-Aided Drug Discovery: A Comparison between In Silico and Crystal Structures of the beta2-Adrenergic Receptor. J Med Chem 2008;51:2907–2914. [PubMed: 18442228]

31. Peleg G, Ghanouni P, Kobilka BK, Zare RN. Single-molecule spectroscopy of the beta(2) adrenergic receptor: Observation of conformational substates in a membrane protein. Proceedings of the National Academy of Sciences of the United States of America 2001;98:8469–8474. [PubMed: 11438704]

32. Park SH, Prytulla S, De Angelis AA, Brown JM, Kiefer H, Opella SJ. High-resolution NMR spectroscopy of a GPCR in aligned bicelles. Journal of the American Chemical Society 2006;128:7402–7403. [PubMed: 16756269]

33. Werner K, Richter C, Klein-Seetharaman J, Schwalbe H. Isotope labeling of mammalian GPCRs in HEK293 cells and characterization of the C-terminus of bovine rhodopsin by high resolution liquid NMR spectroscopy. Journal of Biomolecular Nmr 2008;40:49–53. [PubMed: 17999150]

34. Altenbach C, Cai KW, Klein-Seetharaman J, Khorana FG, Hubbell WL. Structure and function in rhodopsin: Mapping light-dependent changes in distance between residue 65 in helix TM1 and residues in the sequence 306–319 at the cytoplasmic end of helix TM7 and in helix H8. Biochemistry 2001;40:15483–15492. [PubMed: 11747423]

35. Lin SW, Sakmar TP. Specific tryptophan UV-absorbance changes are probes of the transition of rhodopsin to its active state. Biochemistry 1996;35:11149–11159. [PubMed: 8780519]

36. Farrens DL, Altenbach C, Yang K, Hubbell WL, Khorana HG. Requirement of rigid-body motion of transmembrane helices for light activation of rhodopsin. Science 1996;274:768–770. [PubMed: 8864113]

37. Dunham TD, Farrens DL. Conformational changes in rhodopsin. Movement of helix f detected by site-specific chemical labeling and fluorescence spectroscopy. J Biol Chem 1999;274:1683–1690. [PubMed: 9880548]

38. Ruprecht JJ, Mielke T, Vogel R, Villa C, Schertler GF. Electron crystallography reveals the structure of metarhodopsin I. EMBO J 2004;23:3609–3620. [PubMed: 15329674]

39. Vogtherr, M.; Fiebig, K. Modern Methods of Drug Discovery. In: Hillish, A.; Hilgenfeld, R., editors. Birkhauser. 2003. p. 183-202.

40. Homans SW. NMR spectroscopy tools for structure-aided drug design. Angewandte Chemie-International Edition 2004;43:290–300.

41. Ratnala VRP. New tools for G-protein coupled receptor (GPCR) drug discovery: combination of baculoviral expression system and solid state NMR. Biotechnology Letters 2006;28:767–778. [PubMed: 16786240]

42. Nielsen NC, Malmendal A, Vosegaard T. Techniques and applications of NMR to membrane proteins (Review). Molecular Membrane Biology 2004;21:129–141. [PubMed: 15204621]

43. Sanders CR, Sonnichsen F. Solution NMR of membrane proteins: practice and challenges. Magnetic Resonance in Chemistry 2006;44:S24–S40. [PubMed: 16826539]

44. Arshava B, Liu SF, Jiang HL, Breslav M, Becker JM, Naider F. Structure of segments of a G protein-coupled receptor: CD and NMR analysis of the Saccharomyces cerevisiae tridecapeptide pheromone receptor. Biopolymers 1998;46:343–357. [PubMed: 9798427]

45. Berlose JP, Convert O, Brunissen A, Chassaing G, Lavielle S. 3-Dimensional Structure of the Highly Conserved 7Th Transmembrane Domain of G-Protein-Coupled Receptors. European Journal of Biochemistry 1994;225:827–843. [PubMed: 7957220]

46. Arevalo E, Estephan R, Madeo J, Arshava B, Dumont M, Becker JM, et al. Biosynthesis and biophysical analysis of domains of a yeast G protein-coupled receptor. Biopolymers 2003;71:516–531. [PubMed: 14517901]

47. Naider F, Arshava B, Ding FX, Arevalo E, Becker JM. Peptide fragments as models to study the structure of a G-protein coupled receptor: The alpha-factor receptor of Saccharomyces cerevisiae. Biopolymers 2001;60:334–350. [PubMed: 12115145]

48. Estephan R, Englander J, Arshava B, Samples KL, Becker JM, Naider F. Biosynthesis and NMR analysis of a 73-residue domain of a Saccharomyces cerevisiae G protein-coupled receptor. Biochemistry 2005;44:11795–11810. [PubMed: 16128581]

49. Valentine KG, Liu SF, Marassi FM, Veglia G, Opella SJ, Ding FX, et al. Structure and topology of a peptide segment of the 6th transmembrane domain of the Saccharomyces cerevisae alpha-factor receptor in phospholipid bilayers. Biopolymers 2001;59:243–256. [PubMed: 11473349]
50. Zheng HA, Zhao J, Sheng WY, Xie XQ. A transmembrane helix-bundle from G-protein coupled receptor CB2: Biosynthesis, purification, and NMR characterization. Biopolymers 2006;83:46–61. [PubMed: 16634087]
51. Wu JX, Feng M, Ruan KH. Assembling NMR structures for the intracellular loops of the human thromboxane A(2) receptor: Implication of the G protein-coupling pocket. Archives of Biochemistry and Biophysics 2008;470:73–82. [PubMed: 18073117]
52. Demene H, Granier S, Muller D, Guillon G, Dufour MN, Delsuc MA, et al. Active peptidic mimics of the second intracellular loop of the V-1A vasopressin receptor are structurally related to the second intracellular rhodopsin loop: A combined H-1 NMR and biochemical study. Biochemistry 2003;42:8204–8213. [PubMed: 12846569]
53. Mierke DF, Royo M, Pellegrini M, Sun HM, Chorev M. Peptide mimetic of the third cytoplasmic loop of the PTH/PTHrP receptor. Journal of the American Chemical Society 1996;118:8998–9004.
54. Pellegrini M, Mierke DF. Molecular complex of cholecystokinin-8 and N-terminus of the cholecystokinin A receptor by NMR spectroscopy. Biochemistry 1999;38:14775–14783. [PubMed: 10555959]
55. Giragossian C, Mierke DF. Intermolecular interactions between cholecystokinin-8 and the third extracellular loop of the cholecystokinin A receptor. Biochemistry 2001;40:3804–3809. [PubMed: 11300760]
56. Giragossian C, Mierke DF. Intermolecular interactions between cholecystokinin-8 and the third extracellular loop of the cholecystokinin-2 receptor. Biochemistry 2002;41:4560–4566. [PubMed: 11926817]
57. Giragossian C, Sugg EE, Szewczyk JR, Mierke DF. Intermolecular interactions between peptidic and nonpeptidic agonists and the third extracellular loop of the cholecystokinin 1 receptor. Journal of Medicinal Chemistry 2003;46:3476–3482. [PubMed: 12877585]
58. Ulfers AL, Piserchio A, Mierke DF. Extracellular domains of the neurokinin-1 receptor: Structural characterization and interactions with substance P. Biopolymers 2002;66:339–349. [PubMed: 12539262]
59. Ruan KH, Wu JX, So SP, Jenkins LA, Ruan CH. NMR structure of the thromboxane A(2) receptor ligand recognition pocket. European Journal of Biochemistry 2004;271:3006–3016. [PubMed: 15233797]
60. Ruan KH, So SP, Wu JX, Li DW, Huang AM, Kung J. Solution structure of the second extracellular loop of human thromboxane A(2) receptor. Biochemistry 2001;40:275–280. [PubMed: 11141080]
61. Pham TCT, Kriwacki RW, Parrill AL. Peptide design and structural characterization of a GPCR loop mimetic. Biopolymers 2007;86:298–310. [PubMed: 17443712]
62. Kushwaha N, Harwood SC, Wilson AM, Berger M, Tecott LH, Roth BL, et al. Molecular determinants in the second intracellular loop of the 5-hydroxytryptamine-1A receptor for G-protein coupling. Molecular Pharmacology 2006;69:1518–1526. [PubMed: 16410407]
63. Neumann S, Krause G, Claus M, Paschke R. Structural determinants for G protein activation and selectivity in the second intracellular loop of the thyrotropin receptor. Endocrinology 2005;146:477–485. [PubMed: 15498884]
64. Havlickova M, Blahos J, Brabet I, Liu JF, Hruskova B, Prezeau L, et al. The second intracellular loop of metabotropic glutamate receptors recognizes C termini of G-protein alpha-subunits. Journal of Biological Chemistry 2003;278:35063–35070. [PubMed: 12829705]
65. Chung DA, Zuiderweg ERP, Fowler CB, Soyer OS, Mosberg HI, Neubig RR. NMR structure of the second intracellular loop of the alpha 2A adrenergic receptor: Evidence for a novel cytoplasmic helix. Biochemistry 2002;41:3596–3604. [PubMed: 11888275]
66. Piserchio A, Prado GN, Zhang R, Yu J, Taylor L, Polgar P, et al. Structural insight into the role of the second intracellular loop of the bradykinin 2 receptor in signaling and internalization. Biopolymers 2002;63:239–246. [PubMed: 11807751]

67. Jung H, Windhaber R, Palm D, Schnackerz KD. Nmr and Circular-Dichroism Studies of Synthetic Peptides Derived from the 3Rd Intracellular Loop of the Beta-Adrenoceptor. Febs Letters 1995;358:133–136. [PubMed: 7828722]
68. Ulfers AL, McMurry JL, Miller A, Wang LG, Kendall DA, Mierke DF. Cannabinoid receptor-G protein interactions: G(alpha i1)-bound structures of IC3 and a mutant with altered G protein specificity. Protein Science 2002;11:2526–2531. [PubMed: 12237474]
69. Pellegrini M, Bisello A, Rosenblatt M, Chorev M, Mierke DF. Binding domain of human parathyroid hormone receptor: From conformation to function. Biochemistry 1998;37:12737–12743. [PubMed: 9737850]
70. Choi G, Landin J, Xie XQ. The cytoplasmic helix of cannabinoid receptor CB2, a conformational study by circular dichroism and H-1 NMR spectroscopy in aqueous and membrane-like environments. Journal of Peptide Research 2002;60:169–177. [PubMed: 12213126]
71. Choi G, Guo JX, Makriyannis A. The conformation of the cytoplasmic helix 8 of the CB1 cannabinoid receptor using NMR and circular dichroism. Biochimica et Biophysica Acta-Biomembranes 2005;1668:1–9.
72. Katragadda M, Maciejewski MW, Yeagle PL. Structural studies of the putative helix 8 in the human beta(2) adrenergic receptor: an NMR study. Biochimica et Biophysica Acta-Biomembranes 2004;1663:74–81.
73. Jung H, Windhaber R, Palm D, Schnackerz KD. Conformation of a beta-adrenoceptor-derived signal transducing peptide as inferred by circular dichroism and H-1 NMR spectroscopy. Biochemistry 1996;35:6399–6405. [PubMed: 8639586]
74. Franzoni L, Nicastro G, Pertinhez TA, Tato M, Nakaie CR, Paiva ACM, et al. Structure of the C-terminal fragment 300–320 of the rat angiotensin II AT(1A) receptor and its relevance with respect to G-protein coupling. Journal of Biological Chemistry 1997;272:9734–9741. [PubMed: 9092505]
75. Piserchio A, Zelesky V, Yu J, Taylor L, Polgar P, Mierke DF. Bradykinin B2 receptor signaling: Structural and functional characterization of the C-terminus. Biopolymers 2005;80:367–373. [PubMed: 15682437]
76. Lehmann N, Alexiev U, Fahmy K. Linkage between the intramembrane H-bond network around aspartic acid 83 and the cytosolic environment of helix 8 in photoactivated rhodopsin. Journal of Molecular Biology 2007;366:1129–1141. [PubMed: 17196983]
77. Getmanova E, Patel AB, Klein-Seetharaman J, Loewen MC, Reeves PJ, Friedman N, et al. NMR spectroscopy of phosphorylated wild-type rhodopsin: Mobility of the phosphorylated C-terminus of rhodopsin in the dark and upon light activation. Biochemistry 2004;43:1126–1133. [PubMed: 14744159]
78. Kisselev OG, McDowell JH, Hargrave PA. The arrestin-bound conformation and dynamics of the phosphorylated carboxy-terminal region of rhodopsin. Febs Letters 2004;564:307–311. [PubMed: 15111114]
79. Choi G, Landin J, Galan JF, Birge RR, Albert AD, Yeagle PL. Structural studies of metarhodopsin II, the activated form of the G-protein coupled receptor, rhodopsin. Biochemistry 2002;41:7318–7324. [PubMed: 12044163]
80. Yeagle PL, Choi G, Albert AD. Studies on the structure of the G-protein-coupled receptor rhodopsin including the putative G-protein binding site in unactivated and activated forms. Biochemistry 2001;40:11932–11937. [PubMed: 11570894]
81. Yeagle PL, Alderfer JL, Albert AD. Structure of the third cytoplasmic loop of bovine rhodopsin. Biochemistry 1995;34:14621–14625. [PubMed: 7578070]
82. Cai K, Itoh Y, Khorana HG. Mapping of contact sites in complex formation between transducin and light-activated rhodopsin by covalent crosslinking: use of a photoactivatable reagent. Proc Natl Acad Sci U S A 2001;98:4877–4882. [PubMed: 11320237]
83. Cai K, Klein-Seetharaman J, Hwa J, Hubbell WL, Khorana HG. Structure and function in rhodopsin: Effects of disulfide cross-links in the cytoplasmic face of rhodopsin on transducin activation and phosphorylation by rhodopsin kinase. Biochemistry 1999;38:12893–12898. [PubMed: 10504260]
84. Unger VM, Schertler GFX. Low-Resolution Structure of Bovine Rhodopsin Determined by Electron Cryomicroscopy. Biophysical Journal 1995;68:1776–1786. [PubMed: 7612819]

85. Katragadda M, Chopra A, Bennett M, Alderfer JL, Yeagle PL, Albert AD. Structures of the transmembrane helices of the G-protein coupled receptor, rhodopsin. Journal of Peptide Research 2001;58:79–89. [PubMed: 11454172]

86. Tian CL, Breyer RM, Kim HJ, Karra MD, Friedman DB, Karpay A, et al. Solution NMR spectroscopy of the human vasopressin V2 receptor, a G protein-coupled receptor. Journal of the American Chemical Society 2005;127:8010–8011. [PubMed: 15926814]

87. Klabunde T, Hessler G. Drug design strategies for targeting G-protein-coupled receptors. Chembiochem 2002;3:929–944.

88. Surgand JS, Rodrigo J, Kellenberger E, Rognan D. A chemogenomic analysis of the transmembrane binding cavity of human G-protein-coupled receptors. Proteins 2006;62:509–538. [PubMed: 16294340]

89. Jaschke H, Neumann S, Moore S, Thomas CJ, Colson AO, Costanzi S, et al. A low molecular weight agonist signals by binding to the transmembrane domain of thyroid-stimulating hormone receptor (TSHR) and luteinizing hormone/chorionic gonadotropin receptor (LHCGR). Journal of Biological Chemistry 2006;281:9841–9844. [PubMed: 16488885]

90. Moore S, Jaeschke H, Kleinau G, Neumann S, Costanzi S, Jiang JK, et al. Evaluation of small-molecule modulators of the luteinizing hormone/choriogonadotropin and thyroid stimulating hormone receptors: Structure-activity relationships and selective binding patterns. Journal of Medicinal Chemistry 2006;49:3888–3896. [PubMed: 16789744]

91. Hu JX, Jiang JK, Costanzi S, Thomas C, Yang W, Feyen JHM, et al. A missense mutation in the seven-transmembrane domain of the human Ca2+ receptor converts a negative allosteric modulator into a positive allosteric modulator. Journal of Biological Chemistry 2006;281:21558–21565. [PubMed: 16735501]

92. Heitman LH, Oosterom J, Bonger KM, Timmers CM, Wiegerinck PHG, Ijzerman AP. [H-3]Org 43553, the first low-molecular-weight agonistic and allosteric Radioligand for the human luteinizing hormone receptor. Molecular Pharmacology 2008;73:518–524. [PubMed: 17989351]

93. Neumann S, Kleinau G, Costanzi S, Moore S, Jiang JK, Raaka BM, et al. A Low Molecular Weight Antagonist for the Human Thyrotropin Receptor with Therapeutic Potential for Hyperthyroidism. Endocrinology 2008;149:5945–5950. [PubMed: 18669595]

94. Middleton DA. Solid-state NMR spectroscopy as a tool for drug design: from membrane-embedded targets to amyloid fibrils. Biochemical Society Transactions 2007;35:985–990. [PubMed: 17956260]

95. Shuker SB, Hajduk PJ, Meadows RP, Fesik SW. Discovering high-affinity ligands for proteins: SAR by NMR. Science 1996;274:1531–1534. [PubMed: 8929414]

96. Hajduk PJ. SAR by NMR: Putting the pieces together. Molecular Interventions 2006;6:266–272. [PubMed: 17035667]

97. Ballesteros JA, Weinstein H. Integrated methods for the construction of three-dimensional models and computational probing of structure-function relations in G-protein coupled receptors. Methods Neurosci 1995;25:366–428.

98. Eilers M, Reeves PJ, Ying WW, Khorana HG, Smith SO. Magic angle spinning NMR of the protonated retinylidene Schiff base nitrogen in rhodopsin: Expression of N-15-lysine-and C-13-glycine-labeled opsin in a stable cell line. Proceedings of the National Academy of Sciences of the United States of America 1999;96:487–492. [PubMed: 9892660]

99. Grobner G, Burnett IJ, Glaubitz C, Choi G, Mason AJ, Watts A. Observations of light-induced structural changes of retinal within rhodopsin. Nature 2000;405:810–813. [PubMed: 10866205]

100. Creemers AFL, Kiihne S, Bovee-Geurts PHM, Degrip WJ, Lugtenburg J, de Groot HJM. H-1 and C-13 MAS NMR evidence for pronounced ligand-protein interactions involving the ionone ring of the retinylidene chromophore in rhodopsin. Proceedings of the National Academy of Sciences of the United States of America 2002;99:9101–9106. [PubMed: 12093898]

101. Brown MF, Heyn MP, Job C, Kim S, Moltke S, Nakanishi K, et al. Solid-State H-2 NMR spectroscopy of retinal proteins in aligned membranes. Biochimica et Biophysica Acta-Biomembranes 2007;1768:2979–3000.

102. Salgado GFJ, Struts AV, Tanaka K, Fujioka N, Nakanishi K, Brown MF. Deuterium NMR structure of retinal in the ground state of rhodopsin. Biochemistry 2004;43:12819–12828. [PubMed: 15461454]

103. Salgado GFJ, Struts AV, Tanaka K, Krane S, Nakanishi K, Brown MF. Solid-state H-2 NMR structure of retinal in metarhodopsin I. Journal of the American Chemical Society 2006;128:11067–11071. [PubMed: 16925423]
104. Struts AV, Salgado GFJ, Tanaka K, Krane S, Nakanishi K, Brown MF. Structural analysis and dynamics of retinal chromophore in dark and metal states of rhodopsin from H-2 NMR of aligned membranes. J Mol Biol 2007;372:50–66. [PubMed: 17640664]
105. Creemers AFL, Bovee-Geurts PHM, Degrip WJ, Lugtenburg J, de Groot HJM. Solid-state NMR analysis of ligand-receptor interactions reveals an induced misfit in the binding site of isorhodopsin. Biochemistry 2004;43:16011–16018. [PubMed: 15609995]
106. Kiihne SR, Creemers AFL, de Grip WJ, Bovee-Geurts PHM, Lugtenburg J, de Groot HJM. Selective interface detection: Mapping binding site contacts in membrane proteins by NMR spectroscopy. Journal of the American Chemical Society 2005;127:5734–5735. [PubMed: 15839640]
107. Luca S, White JF, Sohal AK, Filippov DV, van Boom JH, Grisshammer R, et al. The conformation of neurotensin bound to its G protein-coupled receptor. Proceedings of the National Academy of Sciences of the United States of America 2003;100:10706–10711. [PubMed: 12960362]
108. Lopez JJ, Shukla AK, Reinhart C, Schwalbe H, Michel H, Glaubitz C. The structure of the neuropeptide bradykinin bound to the human G-protein coupled receptor bradykinin B2 as determined by solid-state NMR spectroscopy. Angewandte Chemie-International Edition 2008;47:1668–1671.
109. Dossey AT, Reale V, Chatwin H, Zachariah C, Debono M, Evans PD, et al. NMR analysis of Caenorhabditis elegans FLP-18 neuropeptides: Implications for NPR-1 activation. Biochemistry 2006;45:7586–7597. [PubMed: 16768454]
110. Ratnala VRP, Kiihne SR, Buda F, Leurs R, de Groot HJM, Degrip WJ. Solid-state NMR evidence for a protonation switch in the binding pocket of the H1 receptor upon binding of the agonist histamine. Journal of the American Chemical Society 2007;129:867–872. [PubMed: 17243823]
111. Ballesteros JA, Jensen AD, Liapakis G, Rasmussen SGF, Shi L, Gether U, et al. Activation of the beta(2)-adrenergic receptor involves disruption of an ionic lock between the cytoplasmic ends of transmembrane segments 3 and 6. Journal of Biological Chemistry 2001;276:29171–29177. [PubMed: 11375997]
112. Shi L, Liapakis G, Xu R, Guarnieri F, Ballesteros JA, Javitch JA. beta2 Adrenergic receptor activation. Modulation of the proline kink in transmembrane 6 by a rotamer toggle switch Journal of Biological Chemistry 2002;277:40989–40996.
113. Altenbach C, Klein-Seetharaman J, Cai K, Khorana HG, Hubbell WL. Structure and function in rhodopsin: mapping light-dependent changes in distance between residue 316 in helix 8 and residues in the sequence 60–75, covering the cytoplasmic end of helices TM1 and TM2 and their connection loop CL1. Biochemistry 2001;40:15493–15500. [PubMed: 11747424]
114. Tikhonova IG, Best RB, Engel S, Gershengorn MC, Hummer G, Costanzi S. Atomistic insights into rhodopsin activation from a dynamic model. Journal of the American Chemical Society 2008;130:10141–10149. [PubMed: 18620390]
115. Patel AB, Crocker E, Eilers M, Hirshfeld A, Sheves M, Smith SO. Coupling of retinal isomerization to the activation of rhodopsin. Proceedings of the National Academy of Sciences of the United States of America 2004;101:10048–10053. [PubMed: 15220479]
116. Crocker E, Eilers M, Ahuja S, Hornak V, Hirshfeld A, Sheves M, et al. Location of Trp265 in metarhodopsin II: Implications for the activation mechanism of the visual receptor rhodopsin. Journal of Molecular Biology 2006;357:163–172. [PubMed: 16414074]
117. Patel AB, Crocker E, Reeves PJ, Getmanova EV, Eilers M, Khorana HG, et al. Changes in interhelical hydrogen bonding upon rhodopsin activation. J Mol Biol 2005;347:803–812. [PubMed: 15769471]
118. Ahuja S, Hornak V, Yan ECY, Syrett N, Goncalves JA, Hirshfeld A, et al. Helix movement is coupled to displacement of the second extracellular loop in rhodopsin activation. Nat Struct Mol Biol 2009;16:168–175. [PubMed: 19182802]
119. Loewen MC, Klein-Seetharaman J, Getmanova EV, Reeves PJ, Schwalbe H, Khorana HG. Solution F-19 nuclear Overhauser effects in structural studies of the cytoplasmic domain of mammalian rhodopsin. Proceedings of the National Academy of Sciences of the United States of America 2001;98:4888–4892. [PubMed: 11320239]

120. Klein-Seetharaman J, Getmanova EV, Loewen MC, Reeves PJ, Khorana HG. NMR spectroscopy in studies of light-induced structural changes in mammalian rhodopsin: Applicability of solution F-19 NMR. Proceedings of the National Academy of Sciences of the United States of America 1999;96:13744–13749. [PubMed: 10570143]

121. Klein-Seetharaman J, Yanamala NVK, Javeed F, Reeves PJ, Getmanova EV, Loewen MC, et al. Differential dynamics in the G protein-coupled receptor rhodopsin revealed by solution NMR. Proceedings of the National Academy of Sciences of the United States of America 2004;101:3409–3413. [PubMed: 14990789]

122. Klein-Seetharaman J, Reeves PJ, Loewen MC, Getmanova EV, Chung L, Schwalbe H, et al. Solution NMR spectroscopy of [alpha-N-15]lysine-labeled rhodopsin: The single peak observed in both conventional and TROSY-type HSQC spectra is ascribed to Lys-339 in the carboxyl-terminal peptide sequence. Proceedings of the National Academy of Sciences of the United States of America 2002;99:3452–3457. [PubMed: 11904408]

123. Mak-Jurkauskas ML, Bajaj VS, Hornstein MK, Belenky M, Griffin RG, Herzfeld J. Energy transformations early in the bacteriorhodopsin photocycle revealed by DNP-enhanced solid-state NMR. Proceedings of the National Academy of Sciences of the United States of America 2008;105:883–888. [PubMed: 18195364]

124. Ulfers AL, McMurry JL, Kendall DA, Mierke DF. Structure of the third intracellular loop of the human cannabinoid 1 receptor. Biochemistry 2002;41:11344–11350. [PubMed: 12234176]

125. Macdonald D, Mierke DF, Li HZ, Pellegrini M, Sachais B, Krause JE, et al. Photoaffinity labeling of mutant neurokinin-1 receptors reveals additional structural features of the substance P/NK-1 receptor complex. Biochemistry 2001;40:2530–2539. [PubMed: 11327875]

126. Piserchio A, Bisello A, Rosenblatt M, Chorev M, Mierke DF. Characterization of parathyroid hormone/receptor interactions: Structure of the first extracellular loop. Biochemistry 2000;39:8153–8160. [PubMed: 10889021]

127. Dorey M, Hargrave PA, McDowell JH, Arendt A, Vogt T, Bhawsar N, et al. Effects of phosphorylation on the structure of the G-protein receptor rhodopsin. Biochimica et Biophysica Acta-Biomembranes 1999;1416:217–224.

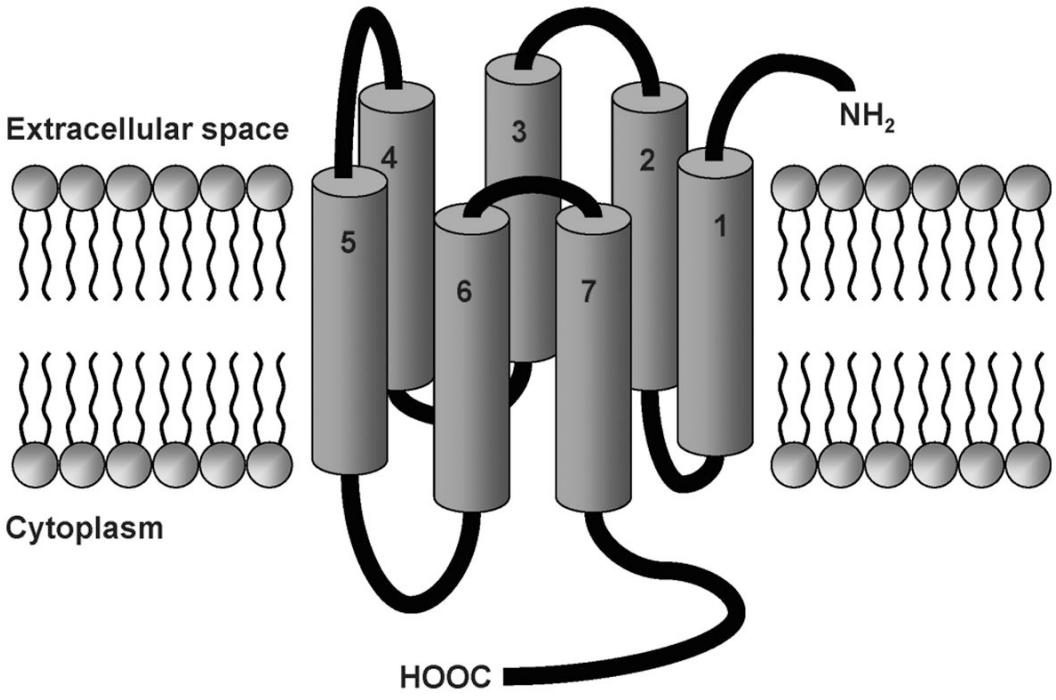

Figure 1.
The topology of G protein coupled receptors.

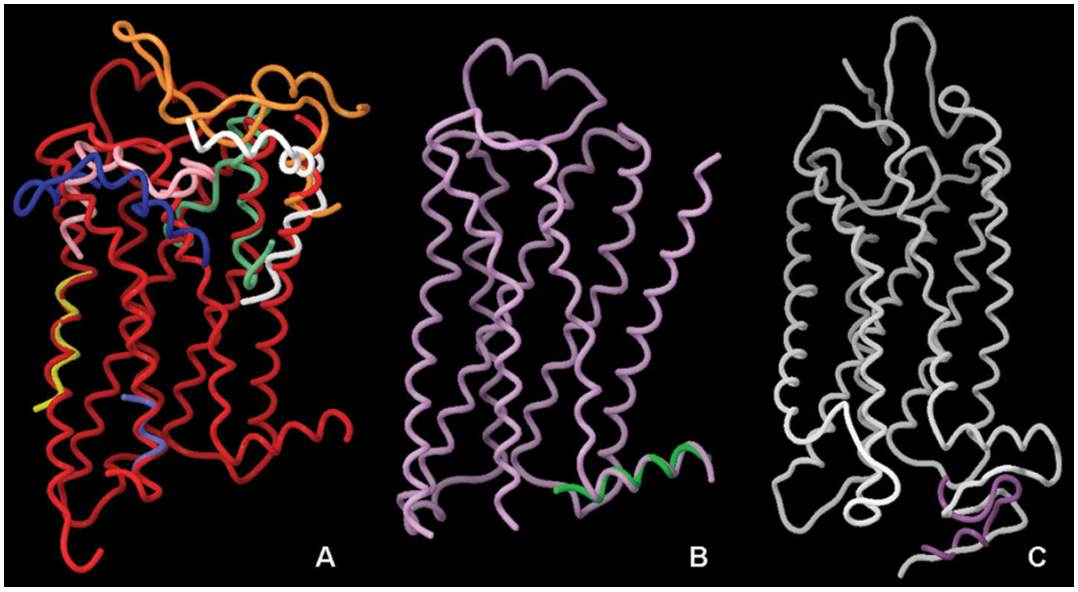

Figure 2.

Structural alignment of the NMR coordinates of GPCR portions deposited in the PDB and the crystal structures of the and bovine rhodopsin. Panel A: superimposition of the β_2-AR crystal structure (2RH1, red) with the NMR-derived structures of the N-termini of PTH_1 (1BL1–white) and CCK_1 (1D6G, orange), EL1 of S_1P_4, (2DCO, aquamarine), IL3 of CB_1 (1LVQ, light blue), TM6 of Ste2pR (1PJD, yellow), and EL3 of CCK_1 (1HZN, pink) and CCK_2 (1L4T, dark blue). Panel B: superimposition of the crystal structure of the β_1-AR (2VT4, plum) with the NMR-derived structure of H8 of the same receptor (1DEP, green). Panel C: superimposition of the crystal structure of rhodopsin (2HPY, white) and the NMR-derived structure of the C-terminus of the same receptor (1NZS, blue purple). Pictures prepared with Maestro 8.0.308, Schrodinger.

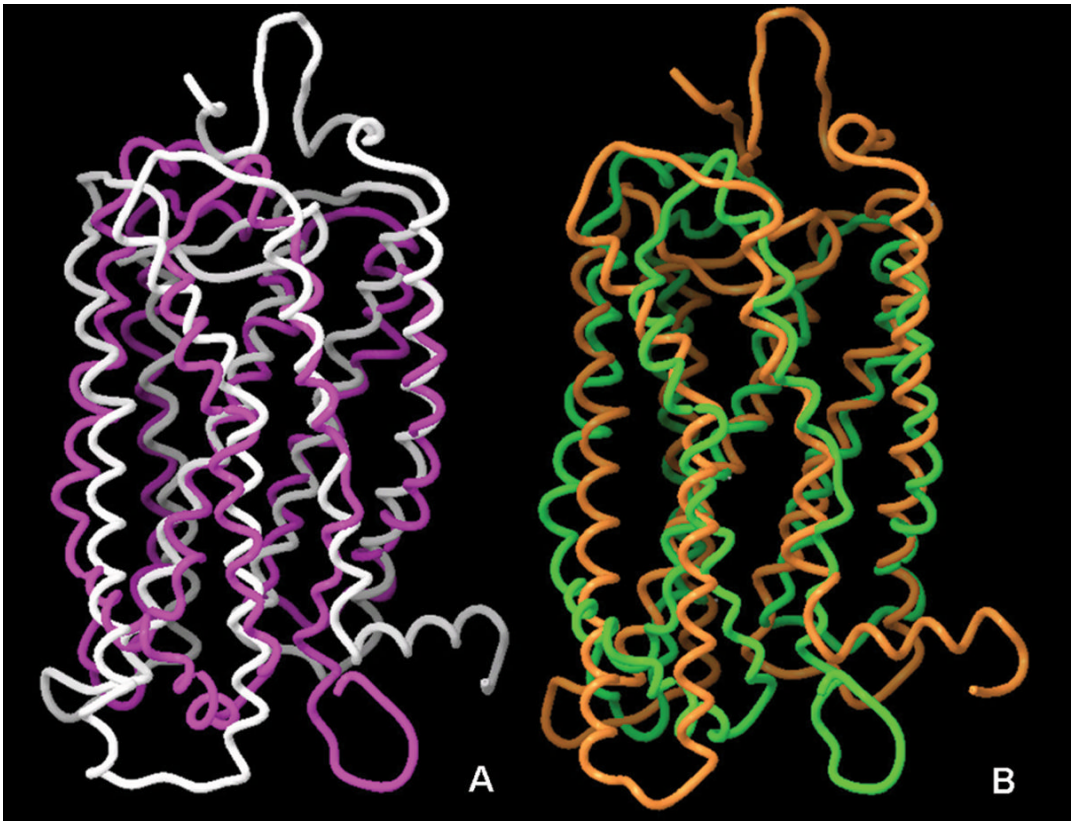

Figure 3.
Superimposition of the crystal structures and the NMR-based three-dimensional models of bovine rhodopsin. Panel A: Superimposition of the X-ray structure (1GZM, white) and the NMR-based model of the ground state (1LN6, purple) receptor. Panel B: Superimposition of the X-ray structure of opsin in its G-protein-interacting conformation (3DQB, orange) and NMR-based model of Meta II rhodopsin (1JFP, green). Picture prepared with Maestro 8.0.308, Schrodinger.

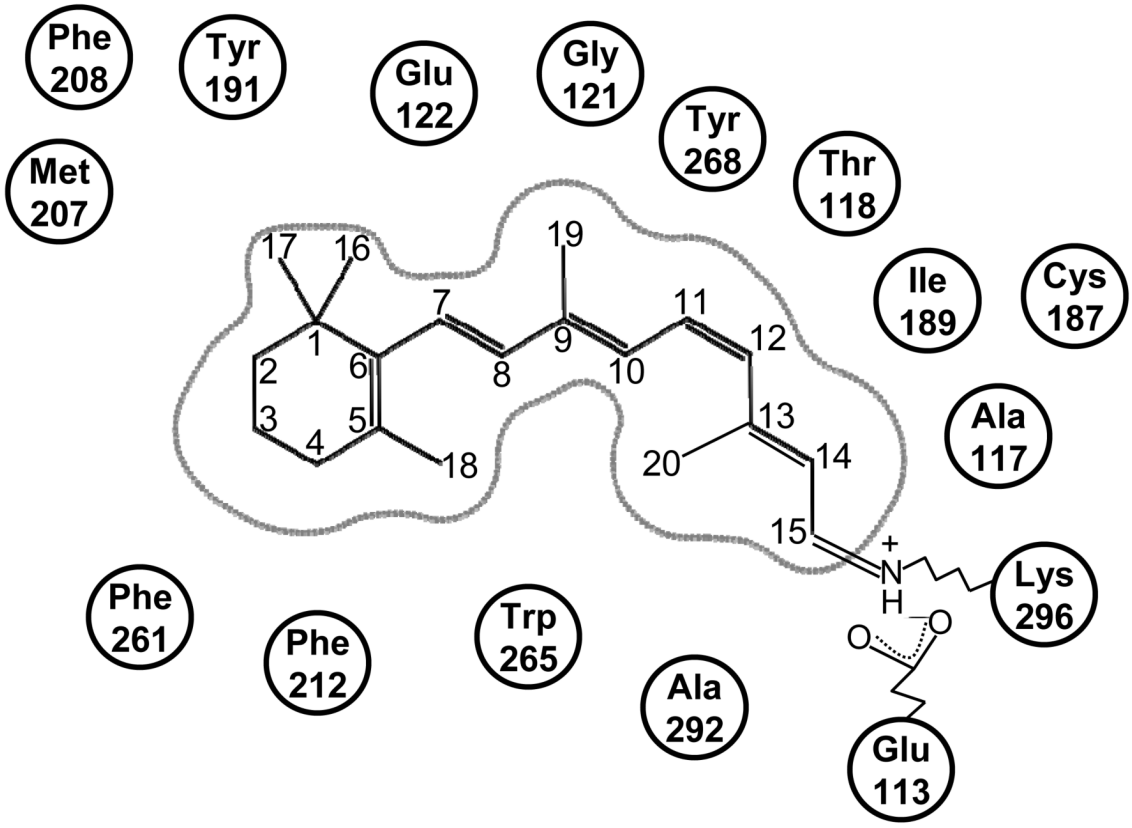

Figure 4.
Two dimensional schematic representation of the retinal binding site in ground state rhodopsin. Picture prepared with MOE 2008.10, Chemical Computing Group.

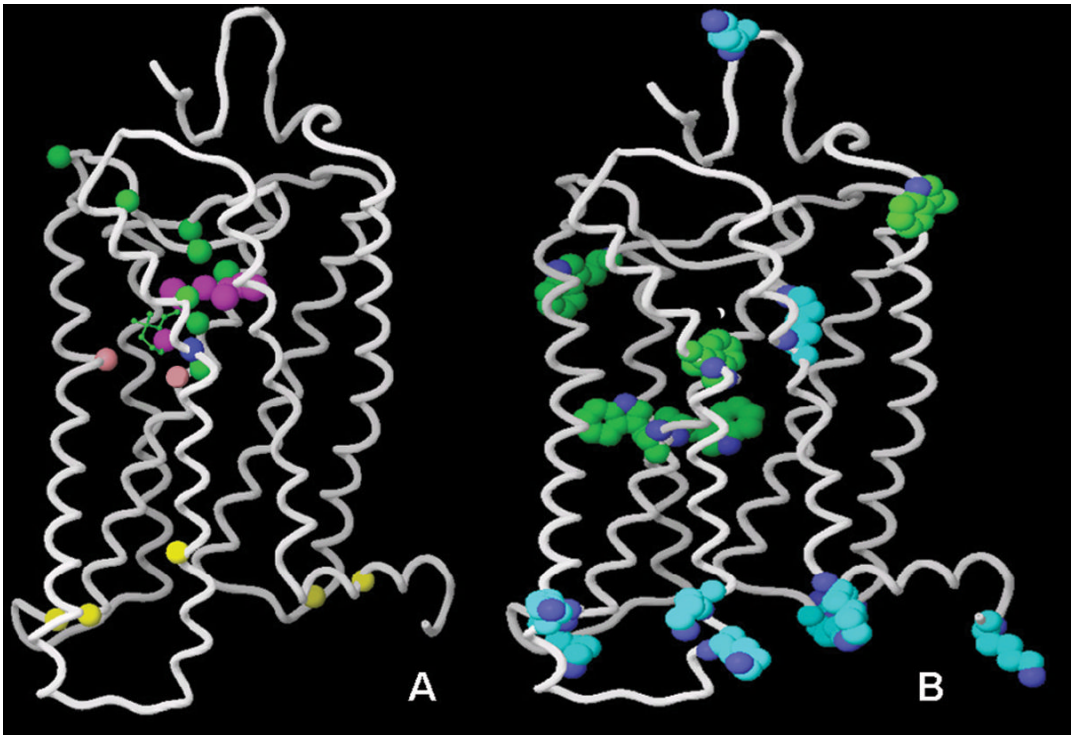

Figure 5.
Panel A: Positions of the ligand atoms and residues labeled in order to study the activation-related conformational changes of rhodopsin. The retinal atoms (C5, C9, C11, C13, C14, C15, C19, C20) are in purple; residues 114, 118, 121, 178, 188, 191, 196, and 268 are in green; residue 265 is in blue; residues 122 and 211 are in pink; the residues mutated to Cys to be labeled with trifluoroethylthio groups are in yellow. For simplicity, only one carbon of the residue backbone is shown. Panel B: All Trp and Lys residues of rhodopsin. Picture prepared with Maestro 8.0.308, Schrodinger.

Table 1

A synoptic view of the available NMR structural data for GPCRs. A list of the abbreviations is provided in footnote[a].

Receptor	Source	Domain	Sequence	Constraints	Solvent	Optimization	Summary of Results	Ref.
α_2 adrenergic receptor	human	TM3-IL2-TM4	121–155	TMA	DPC	DG/EM	120–126: α-helix. 127–131: flexible α-helix. 132–143: α-helix.	[65]
β_2 adrenergic receptor	turkey	IL3	284–295	TMA	LPC TFE AS		290–294: α-helix and flexible Nt in LPC; α-helix in TFE; unstructured in AS; random coil in TFE/AS.	[67]
	human	Helix 8	324–357		AS DMSO DPC	SA/MD	Unstructured in AS. α-helix in DMSO and DPC.	[72]
β_1 adrenergic receptor	turkey	Helix 8	345–359		LMPC DMPC	EM	α-helix (PDB code:1dep).	[73]
AT_{1A} angiotensin receptor	rat	Helix 8	300–320		AS/TFE	SA/MD	306–320: α-helix.	[74]
		IL2	123–156	TMA	DPC-d_{38}	DG/MD	128–139, 147–156: α-helices. 141–145: “U-shape” form.	[66]
B_2 bradykinin receptor	rat	Ct	309–366		DPC		311–326, 333–345, and 348–363: α-helices.	[75]
CB_1 cannabinoid receptor	human	IL3	338–346		AS AS/Gα_{i1}	DG	Unstructured in AS; α-helix with Gα_{i1} (PDB code: 1lvq).	[68]
		IL3	300–343	TMA	SDS	DG/MD	300–310, 312–319 and 332–346: α-helices. 321–327 and 329–331: turns.	[124]
		Helix 8	397–418		AS DPC SDS	SA/MD	Unstructured in AS; α-helix in DPC/SDS.	[71]
CB_2 cannabinoid receptor	human	TM1-IL1-TM2	27–101		DMSO		Preliminary results	[50]
		Helix 8	298–319		AS DMSO DPC	SA/MD	Unstructured in AS; α-helix in DMSO and DPC.	[70]
CCK_1 cholecystokinin receptor	human	Nt EL3	1–47, 329–357 352–379	TMA	DPC/AS	DG/MD MD-wd	1–47: α-helical structures at N- and C-termini and β-sheet stabilized by a disulfide bridge between C18 and C29 (PDB code: 1d6g). 333–337, 341–345, 353–356, 364–367, 372–378: contain helical regions (PDB code: 1hzn).	[54–56]
CCK_2 cholecystokinin receptor	human	EL3	352–379	TMA	DPC/AS	DG/MD-wd	332–339, 341–346, and 351–356: contain helical regions (PDB code: 1l4t).	[56]

Receptor	Source	Domain	Sequence	Constraints	Solvent	Optimization	Summary of Results	Ref.
α-Factor receptor (Ste2pR)	*S. cerevisiae*	TM6	252–269, C252A		TFE/AS	DG/EM	α-helix with a proline kink.	[44]
		TM6	252–269, C252A		DMPC		α-helix with a proline kink (PDB code: 1pjd).	[49]
		TM7, EL3, Cs	267–339		TFE/AS $CDCl_3/CD_3$ H/AS LPC DPC	DG/SA	High helical content of TM7 and Ct in TFE/AS and $CDCl_3/CD_3OH$/AS. Sample stability in detergents was not insufficient for NMR experiments.	[48]
NK_1 Neurokinin receptor	rat	Ns, EL3	1–39, 264–290	TMA	DPC/AS	DG/MD-wd	3–10: α-helix. 264–270: α-helix. 276–289: α-helix.	[58]
		EL2	162–198	TMA	DPC/AS	MD-wd	176–182: α-helix. 187–189: turn.	[125]
PTH_1 parathyroid hormone receptor	human	Nt	168–198	TMA	AS DPC	DG/MD	Low solubility in AS. 170–174, 178–185, and 189–195: contain α-helical structures. 175–177 and 186–188: contain turns (PDB code: 1bl1.pdb).	[69]
		EL1	241–285	TMA	DPC/AS	DG/MD-wd	256–264: α-helix. 275–284: three α-helical loops.	[126]
		IL3	382–408	LF, CF_2	SDS AS	DG	382–393: α-helix with LF and CF_2. 394–398: flexible with CF_2. 394–406: flexible with LF. 402–408: ordered with CF_2. Unstructured in AS.	[53]
Rhodopsin	bovine	TM3-IL2-TM4	125–158	TMA	DPC	DG/EM	125–137: α-helix. 143–146: turn-like structure.	[65]
		Ct	330–348		AS		Unstructured peptide.	[33]
		Phosphorilated Ct	330–348		AS AS/arrestin	DG/MD	Unstructured peptide in AS. The N-terminal portion is flexible and the C-terminal portion assumes a stable helix- loop structure in the presence of arrestin (PDB code: 1nzs).	[77;78;127]
V_{1a} Vaspressin receptor	human	IL2	146–166	LF, CF_1	AS TFE/AS		Random coil conformation in AS; α-helix followed by a β-turn in TFE/AS.	[52]
S_1P_4 Sphingosine 1-phosphate receptor	human	EL1	95–125	DB TMA	AS/TFE	DG/MD	Partially helical structure (PDB code: 2dco).	[61]

Receptor	Source	Domain	Sequence	Constraints	Solvent	Optimization	Summary of Results	Ref.
NK_1 tachykinin receptor		TM7	AMSSTM YNPIISS L		DMSO DMSO/CD Cl_3 PFTB/CD_3 OD	EM/MD	Kinked α-helix as a minor conformer in DMSO; increased folded content in DMSO/$CDCl_3$; twoα-helical regions linked by a hinge around the NP motif in PFTB/CD_3OD.	[45]
A_2 tromboxane receptor	human	EL1	88–104	DB	AS	DG/MD	β-turns.	[59]
		EL2	173–193			DG/MD	A two-turns loop in correspondence of 183 and 188.	[60]
		IL2–3	129–149, 220–246	DB	AS	EM/MD	IL2: large turn. IL3: helical-like conformation.	[51]

[a] AS–aqueous solution; BS–biosynthesis in Escherichia coli; CD–circular dichroism; CF1: cyclized form of peptide with termini substituted by S-carboxymethylcysteine; CF2: cyclized form of the peptide with a linker of 8 methylenes; Ct–C-terminus; DB disulfide bridge; DG–distance geometry; DMPC–deuterated dimyristoyl- phosphatidylcholine; DMSO–dimethyl sulfoxide; DPC dodecylphosphocholine micelles; DQF-COSY–double-quantum filtered correlation spectroscopy; EL–extracellular loop EM–energy minimization; HSQC–Heteronuclear single quantum coherence; IL–intracellular loop; LF–linear form of the peptide; LMPC–deuterated lysomyristoyl-phosphatidylcholine; LPC–1-palmitoyl-2-hydroxy-sn-glycero-3-phosphocholine; MD–molecular dynamics; MD -wd- molecular dynamics in water-decane environment; MS–manual synthesis; NOESY–nuclear overhauser enhancement spectroscopy; Nt–N-terminus; PFTB–perfluoro-*tert*-butanol; PC–Peptide Constrains; SA–simulated annealing; SDS sodium dodecyl sulfate; SF–solid fase automatic synthesis; ssNMR–solid-state NMR; TFE–trifluoroethanol; TM–transmembrane helix; TMA–transmembrane helix anchor; TOCSY–total correlation spectroscopy; TROSY–transverse relaxation optimized spectroscopy.